Special Section: Soil as Complex Systems

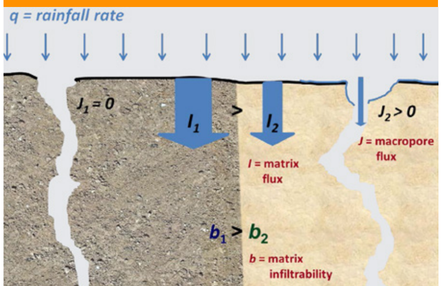

Core Ideas:

- Preferential flow can be predicted from the distribution of mesoscale matrix infiltrability.
- Soil matrix material, rather than the characteristics of macropores, largely controls preferential flow.
- Two different scales of representative areas are needed to predict matrix–macropore partitioning.

John R. Nimmo, USGS, 345 Middlefield Rd., MS-420, Menlo Park, CA 94025 USA (jrnimmo@usgs.gov).

Vadose Zone J.
doi:10.2136/vzj2015.05.0079
Received 22 May 2015.
Accepted 4 Oct. 2015.

Quantitative Framework for Preferential Flow Initiation and Partitioning

John R. Nimmo

A model for preferential flow in macropores is based on the short-range spatial distribution of soil matrix infiltrability. It uses elementary areas at two different scales. One is the traditional representative elementary area (REA), which includes a sufficient heterogeneity to typify larger areas, as for measuring field-scale infiltrability. The other, called an elementary matrix area (EMA), is smaller, but large enough to represent the local infiltrability of soil matrix material, between macropores. When water is applied to the land surface, each EMA absorbs water up to the rate of its matrix infiltrability. Excess water flows into a macropore, becoming preferential flow. The land surface then can be represented by a mesoscale (EMA-scale) distribution of matrix infiltrabilities. Total preferential flow at a given depth is the sum of contributions from all EMAs. Applying the model, one case study with multi-year field measurements of both preferential and diffuse fluxes at a specific depth was used to obtain parameter values by inverse calculation. The results quantify the preferential–diffuse partition of flow from individual storms that differed in rainfall amount, intensity, antecedent soil water, and other factors. Another case study provided measured values of matrix infiltrability to estimate parameter values for comparison and illustrative predictions. These examples give a self-consistent picture from the combination of parameter values, directions of sensitivities, and magnitudes of differences caused by different variables. One major practical use of this model is to calculate the dependence of preferential flow on climate-related factors, such as varying soil wetness and rainfall intensity.

Abbreviations: EMA, elementary matrix area; PFF, preferential flow fraction; REA, representative elementary area; STVF, surface-tension viscous flow; VF, viscous flow.

When water is applied to the land surface, it is important to know whether and how much of it goes into the subsurface as preferential flow. Fundamentally, preferential flow travels significant distances along preferred paths that constitute a small fraction of the medium's volume. Faster and less interactive with solid material than diffuse flow (Gerke, 2006; Jarvis, 2007), preferential flow is important to aquifer recharge rates, contaminant transport, soil–plant–water relations, salt and nutrient distributions in the root zone, hydromechanical phenomena such as landslides, and subsurface stormflow. Practical needs concerning preferential flow include a means of predicting its initiation, and the quantitative partitioning of flowing water into diffuse and preferential modes.

Major influences on preferential flow include relatively stable factors, such as the medium and its hydraulic properties, and time-varying hydraulic conditions, such as the soil water content and the source of applied water (Heppell et al., 2002). Different flow behaviors arise from water sources that are uniform or concentrated in space or intensities that are low or high (Beven and Germann, 1982; Pruess, 1999). Criteria for recognizing and predicting preferential flow must account for diverse nonequilibrium processes and a wide range of moisture states (Thomas and Phillips, 1979; Hendrickx and Flury, 2001; Jarvis, 2007). Types of preferential flow include macropore flow (Aubertin, 1971), funneled flow (Kung, 1990), and fingered or unstable flow (Hendrickx and Flury, 2001). This study emphasizes macropore flow, which often can include the greatest portion of preferential flow, and whose quantitative representation may also serve for other flow modes.

For initiation of macropore flow by water applied at the land surface, this study uses the criterion that water enters macropores when the input rate (as from precipitation, irrigation, snowmelt, or other sources) exceeds the infiltrability of the surrounding matrix (Beven and Germann, 1982). Various researchers have used this or similar criteria (e.g., Bronstert and Plate, 1997; Kätterer et al., 2001; Dusek et al., 2008). Certain other commonly used criteria, like saturation of matrix or complete filling of macropores, constitute a special case of this more inclusive criterion, and so do not have to be considered separately. It is important not to assume that matrix saturation is required. Accumulated evidence (e.g., Aubertin, 1971; Quisenberry and Phillips, 1976; Scotter and Kanchanasut, 1981; Andreini and Steenhuis, 1990; Hardie et al., 2013), reviewed by Nimmo (2012) and Villholth et al. (1998), shows that preferential flow is commonplace in soils whose moisture states are substantially less than saturated. Preferential flow may be greater in drier media. In cracking soils, for example, macropores are largest when the soil is dry. Hydrophobicity, which also can cause flow to be preferential (Ritsema and Dekker, 1996), tends to be greater in drier soil.

Observations also show that hydrologically significant preferential flow can occur in macropores that are partially water filled, that is, that air as well as water occupies their internal space. Pore aperture then has much less importance, and the preferential fluxes do not depend on the saturated hydraulic conductivity (Radulovich et al., 1992). Experimental investigations, including those of Su et al. (1999, 2003), Dragila and Weisbrod (2003), and Cey and Rudolph (2009), have observed this effect. Further evidence comes from the general trend of field-measured speeds of preferential flow (Nimmo, 2007) toward values that are seldom fast enough to be explainable as gravity-driven Poiseuille flow through capillary diameters of the size normally reckoned as macropores. This limited speed of preferential flow is what leads to the calculation of small (tens of micrometers or less) effective conduit diameters in studies such as those of Kung et al. (2005) and Germann and Hensel (2006). Investigators, including Tokunaga et al. (2000), Tuller and Or (2001), Hincapié and Germann (2009), and Nimmo (2010), have developed models based on pores that are partially filled with water.

Research on preferential flow has always recognized, at least implicitly or qualitatively, the importance of the partitioning between macropore and matrix modes of flow. One way to quantify this partitioning is with a preferential flow fraction (PFF), defined as the fraction of input water that at a given time is undergoing preferential flow. Alternatives exist, although in this work I emphasize the PFF for a specific depth at which preferential flow occurs. This quantification has considerable utility in applications from hydrology, agriculture, waste disposal, ecohydrology, and other fields (e.g., Heppell et al., 2002; van Schaik et al., 2008; Perkins et al., 2011).

One way to estimate PFF uses measured resident concentrations of a conservative tracer in soil some time after its application at the land surface (Tyner et al., 2007; Perkins et al., 2011). Subsurface drainage from agricultural fields may provide data for PFF flux (e.g., Villholth and Jensen, 1998; Kohler et al., 2003). Hillslope-runoff investigations can also produce analogous quantities (e.g., Bronstert and Plate, 1997; Bronstert, 1999; Stone et al., 2008).

Previous research on the initiation and partitioning of preferential flow notably includes the model of Weiler and Naef (2003). Their Eq. [3] takes macropore inflow to be proportional to the difference between an applied rate of input and a maximum absorption limit of soil matrix material, as discussed above. Weiler and Naef emphasize microtopography, and the area of soil that feeds macropores. The model of Weiler (2005) has similarities, though differing in that it relies to some extent on conditions of pondedness and specific macropore properties. While not explicitly centered on macropore flow, the infiltration investigations of Langhans et al. (2011, 2013) explored increases of infiltrability with increasing rainfall intensity. They developed concepts related to the role of small-scale heterogeneity, utilizing the relation between localized heterogeneity and larger-scale infiltrability developed by Hawkins and Cundy (1987) for runoff quantification.

Specific objectives of this paper are to identify criteria for the initiation of macropore flow at the land surface, and to develop a means of estimating the preferential flow fraction, based on spatially variable soil properties, conditions, and the applied flux density. Emphasis is on areally uniform rainfall, although the framework applies to irrigation, ponding, or other input modes as well. Tests with measured data evaluate this framework's ability to realistically connect soil and storm characteristics with PFF, and the practicality of its implementation.

Framework for Partitioning of Land–Surface Input

Definitions and Description

Matrix and Macropore

The soil matrix, which occupies most of the soil's volume, has numerous pores of limited extent, for convenience called micropores. In these pores, surface tension[1] can create an effective driving force, supplemental to gravity, expressed as the gradient of matric potential. Flow within the matrix is assumed to occur under surface-tension viscous-flow (STVF) conditions, in which both gravity and matric potential gradients are significant for driving flow (Miller and Miller, 1956; Yang et al., 1988).

[1] In similar contexts, the commonly used but less general term is capillarity, the expression of surface tension for water surrounded by the walls of a rigid conduit.

In the range of moderate to high water contents, surface tension or capillary forces exert a major effect on the fullness of individual pores, in addition to generating driving force. For example, by Haines jumps, pores toggle abruptly between a state of little water with essentially negligible conductance, and a state of near fullness, with relatively large conductance. This toggling leads to the common generalization that only the full pores contribute significantly to flow.

Large aperture is a typical reason for a pore to function as a macropore. Natural features like shrink–swell cracks, wormholes, and rootholes can constitute preferential flow paths (e.g., Beven and Germann, 1982; Coppola et al., 2012), but the correspondence between such observable features and hydraulically effective preferential flow paths is not complete or exact. Some wide pores are ineffective flow paths because of poor connectivity. Some small-aperture pores effectively convey preferential flow because they have long-range extent and good connectivity (Bouma, 1981). Evidence suggests that downward-streaming water in forms such as films and rivulets of thickness that may be a few 10s of micrometers or less, can convey significant preferential flow (Kung et al., 2005, 2006; Germann and Hensel, 2006; Nimmo, 2010). Because such streams do not fill the entire pore cross-section, aperture-based criteria do not apply. Micropores, being composed of the spaces between individual grains, naturally do not extend (in the flow direction) much more than a single grain diameter. To transmit preferential flow, macropores necessarily have lengths many times greater than one grain diameter.

For a wide pore that is completely water filled, capillarity is not a major driving force because its influence goes inversely with aperture size. For a wide or narrow macropore that is incompletely water filled, capillarity is likewise not a major influence because the air–water interfaces do not extend across the aperture. Thus preferential flow in macropores is driven predominantly by gravity, with capillary forces (hence matric potential gradients) being relatively insignificant for flow in the direction of the path. (Capillary forces may, however, be significant in a perpendicular direction, as for absorption into the matrix.) A macropore, then, functions under viscous-flow (VF) but not STVF conditions.

For these reasons I adopt here a functional definition. A macropore that conveys preferential flow is one in which gravity is the dominant driving force and substantial flow can be conveyed when the pore is incompletely water filled. The aperture can be small, possibly <100 μm, but the continuous length must be many grain-diameters long. Though not directly inclusive of fingered or unstable flow, which are conveyed by a collection of adjacent pores, this definition would typically include a large portion of preferential flow that occurs in soils and rocks.

Flow Path

Initiation of preferential flow may occur at the land surface, as emphasized here. Alternatively, it could be at an injection well, a perched water body that supplies water to unsaturated material below, or a subsurface feature where water seeps from matrix to macropore. The model in this paper could be readily adapted for such alternatives. Water that travels preferentially to a specified depth is typically a fraction of the preferential flow initiated at the land surface, because of macropore termination, matrix absorption, or other reasons. Dye-tracer experiments often show these effects (e.g., van Schaik, 2009), and they have been treated quantitatively by Nimmo and Mitchell (2013) in terms of varying matrix water content at depths where domain transfer occurs. A rigorous treatment of PFF needs specific consideration of the depth of interest, the choice of which depends on the application at hand.

Characterization of the Land Surface

The land surface is conceived predominantly as exposed, heterogeneous matrix. In this sense, matrix material also includes rock outcrops or other virtually nonconductive features. The area of macropore openings at the land surface typically would be negligible.

For separate treatment of matrix and macropore infiltration, two levels of elementary areas require consideration. One is the commonly recognized representative elementary area (REA) of land surface. It must include a representative sample of macropores as well as of the heterogeneous matrix material. Its size depends on land-surface attributes, at minimum being large enough that a measurement of infiltrability, or infiltration capacity, over this area would not differ significantly from a measurement over a somewhat larger area within the same plot. To include a representative distribution of macropores might require it to be several square meters or more. Infiltrability measurements often are done over a smaller area, thus requiring numerous measurements combined with appropriate averaging techniques to estimate the infiltrability of the REA and hence of the larger plot (e.g., Wilson and Luxmoore, 1988; Nimmo et al., 2009; Perkins et al., 2011).

The other important elementary area is a localized representative area appropriate for characterizing the matrix material, here called an elementary matrix area (EMA). It must be large enough to include many micropores, so as to have measureable soil hydraulic properties, and small enough to exclude macropores. It is not intended to represent an area larger than itself. Thus in terms of unsaturated-zone hydrology, the EMA is a mesoscale concept. It can feed localized runoff or infiltrating water to a macropore entry point. The EMA has similarities to other concepts of a localized water-collecting area, such as the macropore drainage area (MDA) of Weiler and Naef (2003). In a quantitative field-scale preferential flow model, it is a convenience to assume that EMAs are effectively infinitesimal. This allows development in terms of a continuous distribution of EMAs within the REA and is employed here. Each

EMA has a matrix infiltrability, b, the maximum flux density [L T^{-1}] of input that the EMA can completely absorb directly into the matrix material. Besides varying spatially within the REA, b varies temporally with local water content and possibly other factors.

A statistically significant number of measurements could quantify the spatial distribution of b. Such values could be inferred from measurements of the infiltrability of individual aggregates. An infiltrometer small enough to exclude the influence of macropores (Hallett et al., 2004; Lipiec et al., 2009) also could indicate b. One might also employ a larger tension infiltrometer with applied tension adjusted appropriately to exclude macropore flow (e.g., Wilson and Luxmoore, 1988; Jarvis et al., 2013). Indirect determinations also might be practical, such as the inference of localized infiltrability from microtopography (Langhans et al., 2013).

Flow Processes

Sub-REA and REA scales

At an EMA, input water infiltrates into matrix up to the infiltrability of the EMA:

$$\begin{aligned} i &= q, \quad q \le b \\ &= b, \quad q > b \end{aligned} \qquad [1]$$

where i is the infiltration flux density into the matrix material, and q is the flux density of input water applied to the EMA. Excess water (w) left over from matrix infiltration then is

$$\begin{aligned} w &= 0, \quad q \le b \\ &= q - b, \quad q > b \end{aligned} \qquad [2]$$

Entry into macropores is based on an assumption that this excess water has immediate access to a macropore entry point, as if adjacent to it. This assumption is not restricted to any particular process that feeds the macropore. Localized overland flow is one plausible process. Another is that after infiltrating a short distance, perhaps a few millimeters or less, water may move laterally in shallow matrix material (Ritsema and Dekker, 1995). Such lateral flow might occur because the matrix immediately beneath it has extremely low K due to dryness, hydrophobicity, or other factors. It would be analogous to lateral movement of water immediately above the wetting front during conditions of saturation overshoot (Shiozawa and Fujimaki, 2004).

With this assumption that the excess from all EMAs is collectively available to macropores, the total effective excess for the REA is

$$w_{\text{eff}} = \frac{1}{A}\iint_{\text{REA}} max(q-b,0)\,\mathrm{d}s \qquad [3]$$

where A is the area of the REA, s is a dummy variable of dimension L^2, and the function max(x,y) designates the greater of x and y. In the absence of long-range runoff (beyond the REA), w_{eff} would flow into macropores. Figure 1 illustrates this matrix–macropore partitioning for hypothetical contrasting matrix materials.

The macropores within a REA have a collective infiltrability, c, in terms of total volumetric flux per unit area of REA, which indicates the maximum rate of supplied water that the macropores can accept for preferential flow. In general c varies in time, for example with changes in shrink–swell cracks. Available water in excess of c becomes long-range runoff. Because excess input from EMAs flows into macropores of the REA up to the value of c,

$$\begin{aligned} j &= w_{\text{eff}}, \quad w_{\text{eff}} \le c \\ &= c, \quad w_{\text{eff}} > c \end{aligned} \qquad [4]$$

where j is the infiltration flux density into the macropores, collectively, of an REA. The excess over the combined capacities of the matrix and macropores of the REA becomes local ponding or runoff. Thus the runoff per unit area r from an REA is

$$\begin{aligned} r &= 0, \quad w_{\text{eff}} \le c \\ &= w_{\text{eff}} - c, \quad w_{\text{eff}} > c \end{aligned} \qquad [5]$$

REA and Larger Scales

Large-scale dynamics take into account such EMA characteristics as the spatial variability of localized infiltrability. The total infiltrability at the REA scale (symbolized i_{tot}) equals the macropore infiltrability plus an effective matrix infiltrability b_{eff}:

$$i_{\text{tot}} = c + b_{\text{eff}} = c + \frac{1}{A}\iint_{\text{REA}} b\,\mathrm{d}s \qquad [6]$$

At the REA scale, b_{eff} is the average of the EMA-scale b values.

Using continuum representations of both b and c over the land area, the bivariate distribution function $h(b,c)$ [T^2 L^{-2}] can represent properties such that $h(\hat{b},\hat{c})\mathrm{d}b\mathrm{d}c$ is the relative abundance of area having

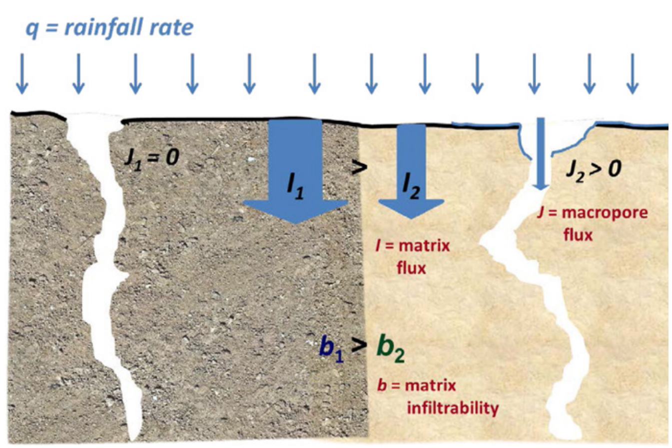

Fig. 1. Macropore flow initiation, comparing adjacent parcels of soil that differ in matrix infiltrability.

$$\hat{b} \le b < \hat{b} + \mathrm{d}b$$
$$\hat{c} \le c < \hat{c} + \mathrm{d}c \quad [7]$$

The function h is normalized such that

$$\int_0^\infty \int_0^\infty h(b,c)\ \mathrm{d}c\ \mathrm{d}b = 1 \quad [8]$$

This function is analogous to bivariate distribution functions used by Philip (1964) and Mualem (1974) for pore-scale properties. It could be represented by a cloud of probability density in two-dimensional bc space.

To compute a property applicable over a particular area, $h(b,c)$ is integrated, weighted by the expression of that property, over the appropriate region of bc space. This procedure is closely analogous to that of Hawkins and Cundy (1987) for a univariate distribution of infiltration capacity. The effective matrix infiltration flux density over the REA is

$$i_{\mathrm{eff}} = \int_0^\infty \int_0^\infty i h(b,c) \mathrm{d}c \mathrm{d}b = \int_0^q \int_0^\infty b h(b,c) \mathrm{d}c \mathrm{d}b + q \int_q^\infty \int_0^\infty h(b,c) \mathrm{d}c \mathrm{d}b \quad [9]$$

The collective macropore infiltration flux density over the REA is

$$j = \int_0^q \int_0^{q-b} c h(b,c) \mathrm{d}c \mathrm{d}b + \int_0^q \int_{q-b}^\infty (q-b)\ h(b,c) \mathrm{d}c \mathrm{d}b \quad [10]$$

Runoff per unit area of REA is

$$r = \int_0^q \int_0^q (q-b-c)\ h(b,c) \mathrm{d}c \mathrm{d}b \quad [11]$$

Thus, at a given time these formulas predict the partitioning of input q into matrix infiltration, preferential flow, and runoff. Note also that w_{eff} can be calculated as

$$w_{\mathrm{eff}} = j + r = \int_0^q \int_0^\infty (q-b)\ h(b,c) \mathrm{d}c \mathrm{d}b \quad [12]$$

These predictions require a known valuation of $h(b,c)$, that is, the distribution of matrix infiltrability and macropore infiltrability, to characterize the land surface at a given time. Matrix infiltrability could likely be determined as noted above in the section on land-surface characterization. For macropore infiltrability, c, the measurement is not as straightforward because it involves numerous macropores that are separated in space. Given a measurement of b_{eff} and i_{tot} over a suitably large area, Eq. [6] can be applied to give c by subtraction. A parameterized $h(b,c)$ could be calculated by inverse modeling from field measurements, though an extensive data set would be required, ideally with separate i_{eff}, j, and r values for a range of q.

For practicality of application and testing within the scope of this study, from here on this paper considers the limiting case of large c, such that there is no runoff. In this case the univariate distribution function

$$g(b) = \int_0^\infty h(b,c) \mathrm{d}c \quad [13]$$

can represent the needed land-surface properties. This restricted model can separately predict the partitioning of infiltration into matrix and macropore components in the many situations where runoff is negligible. The matrix infiltration flux density is

$$i_{\mathrm{eff}} = \int_0^q b\, g(b) \mathrm{d}b + q \int_q^\infty g(b) \mathrm{d}b \quad [14]$$

and the macropore infiltration flux density is

$$j = q - i_{\mathrm{eff}} = \int_0^q (q-b)\, g(b) \mathrm{d}b \quad [15]$$

Figure 2 shows a graphical interpretation of Eq [14] and [15] applied at a given time, when rainfall intensity has the value q. The value of $g(b)$ is proportional to the abundance of area within the REA that has matrix infiltrability b. Where $b > q$, all input water goes to matrix flow, given by the second integral on the right side of Eq. [14] and labeled as Region I in the figure. For the range

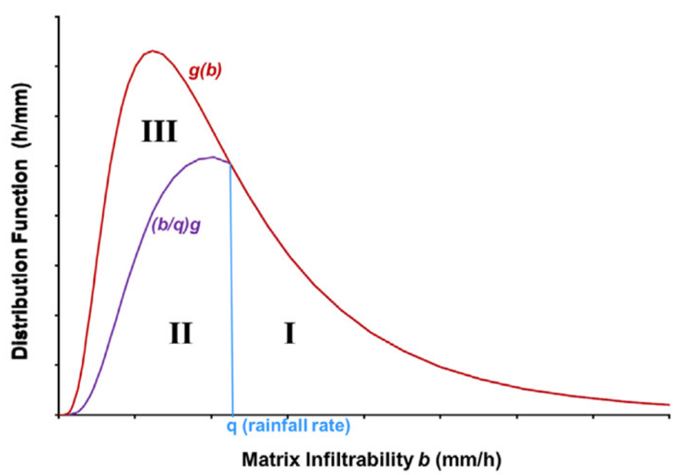

Fig. 2. Hypothetical distribution of matrix infiltrability $g(b)$, within a representative elementary area of soil. Given rainfall at a rate q, the flow-partitioning framework in this paper divides the area under the $g(b)$ curve into three regions. A suitably weighted integration of Areas I and II predicts the effective matrix infiltration flux density as in Eq. [14], and of Area III predicts the effective macropore infiltration flux density as in Eq. [15].

of $b < q$, at each value of b, a fraction b/q of the input flux density goes to matrix infiltration, and the remainder to macropores. This distinction divides this range into two regions of integration, separated by the curve $(b/q)g(b)$. Below this curve, Region II represents matrix infiltration, the first integral on the right side of Eq. [14]. Above this curve, Region III represents macropore infiltration, the integral in Eq. [15].

The distribution function $g(b)$ can be parameterized for convenience. Examples in this paper employ a lognormal distribution, as commonly used for hydraulic conductivity distributions (e.g., Nielsen et al., 1973; Smith and Hebbert, 1979; Patin et al., 2012):

$$g(b)=\frac{1}{b\sigma_g\sqrt{2\pi}}\exp\left[-\frac{\left(\ln(b)-\mu_g\right)^2}{2\sigma_g^2}\right] \qquad [16]$$

Two parameters represent the distribution of b values: μ_g, the geometric mean of the distribution, and σ_g, its geometric standard deviation. The calculation of $g(b)$ from a hypothetical or fitted distribution of b values thus can be calculated by computing the normalized lognormal probability function at each b value and dividing by b.

Case-Study Testing and Applicability

Purpose and Requirements

Without known values of the $g(b)$ function, a fully predictive test of PFF estimation is not possible. The objective here instead is to show how the developed framework provides a basis for relating the occurrence and quantity of preferential flow to soil hydraulic properties, soil water conditions, and rainstorm characteristics. The first case study, using measured data suitable for evaluation of $g(b)$ by inverse modeling, infers the relative importance of critical variables that influence preferential flow to evaluate the consistency of the overall picture that emerges and the reasonableness of optimized parameter values. The second uses field measurements of spatially varying matrix infiltrability to show how the model predicts the amount of preferential flow as a function of storm intensity.

Data required for inverse calculation of $g(b)$ include the water input rate $q(t)$ and preferential flux density $j(t)$ through a subsurface plane for a range of conditions. Such measurements could come from experiments using field-drainage outflow (e.g., Kung et al., 2005; Rosenbom et al., 2010) or water table fluctuation (Salve et al., 2012), though it is rare to find the full range of data types needed. Eguchi and Hasegawa (2008) published an unusually complete data set, measured with a water balance, Darcian flux technique, used here for inverse modeling of $g(b)$. Instruments included a rain gauge for $q(t)$, TDR probes for soil water content, and tensiometers for matric potential. Eguchi and Hasegawa (2008) recorded data from an agricultural field in Tsukuba, Japan at 0.5-h intervals. They calculated matrix flow $i(t)$ at the 1-m depth with Darcy's Law, using $\theta(t)$ measured at 1-m depth, $K(\theta)$ previously measured on core samples from that depth, and matric potential gradient computed from tensiometer measurements at depths of 0.90 and 1.10 m. They determined soil water storage $S(t)$ from TDR measurement of average θ within the 0- to 1-m depth interval. By water-balance considerations, preferential flow $j(t)$ at 1-m depth was computed as

$$j(t)=q(t)-i(t)-\frac{dS}{dt} \qquad [17]$$

In their 7 yr of data, Eguchi and Hasegawa (2008) found 26 rainstorms that generated significant preferential flow.

Data for forward calculation of $g(b)$ are available from the investigation of Wilson and Luxmoore (1988). At 37 locations in a forested watershed in eastern Tennessee, USA, they measured the near-surface hydraulic conductivity under conditions of slight suction, interpreted as matrix infiltrability. A lognormal fit to the relative abundance of data as a function of the infiltrability gives a usable $g(b)$ function. Although no measurements of preferential flow are available to compare with model predictions, the model outputs can be compared with those obtained with the Eguchi and Hasegawa data set to further evaluate the model's usefulness and ability to generate a self-consistent and plausible quantification of preferential flow behavior.

Procedure

Application of the model with the data of Eguchi and Hasegawa (2008) is done on a storm-by-storm basis, as opposed to an instantaneous or fixed time-interval basis. A single storm includes multiple 0.5-h timesteps that each may have a different amount of rain, and hence a different q. For analysis of a storm by the method diagrammed in Fig. 2, this raises the question of what q best characterizes it. One alternative is the average intensity q_{avg}:

$$q_{avg}=\frac{1}{n\delta t}\sum_{i=1}^{n}R_i \qquad [18]$$

where the storm lasts for n timesteps of duration δt in which the amount of precipitation is R_i [L]. This would give a relatively small value, with little relative influence of the timesteps of greatest precipitation, which possibly have the greatest real effect. Another alternative is to use the maximum intensity $R_m/\delta t$, where m indexes the timestep of greatest R_i. This would give a larger value, though it neglects any influence of the rest of the storm's precipitation. A compromise used here is an intensity-weighted average. The precipitation of each timestep is weighted by the ratio of its intensity $R_i/\delta t$ to the average intensity

$$q_{wtd}=\frac{1}{n\delta t}\sum_{i=1}^{n}R_i\left(\frac{\frac{R_i}{\delta t}}{q_{avg}}\right)=\frac{\sum_{i=1}^{n}R_i^{\,2}}{\delta t\sum_{i=1}^{n}R_i} \qquad [19]$$

This value falls between q_{avg} and $R_m/\delta t$ and retains some sensitivity to the overall storm magnitude and average intensity, while being especially sensitive to the timesteps of greatest intensity.

Optimization for the calibration of parameters μ_g and σ_g of the lognormal distribution (Eq. [16]) is based on the objective of matching the given storm's model-calculated PFF to Eguchi and Hasegawa's measured value. Of the two lognormal-distribution parameters, it is necessary to vary only one, since we are optimizing to a single scalar value. The one chosen here is μ_g, which lends itself easily to an intuitive physical interpretation through its relation to the average b value. This leaves the geometric mean σ_g to be assigned a value. This parameter is interpretable as the factor that μ_g would be multiplied or divided by to be one standard deviation away from the geometric mean. It must be greater than 1, which would give an infinitely narrow distribution. Too large a value would smear distributions out too flat on the b axis. The illustrations here use a value of 3.0 as a compromise that produces visually reasonable distributions. This choice is further evaluated below in terms of sensitivities and comparison to other data.

Results

Test with Known Values of PFF

For testing, five storms were chosen from the Tsukuba data set of Eguchi and Hasegawa. Designated by year-month-day of the start of the storm, these are:

- Storm 2001-10-10, the example highlighted by Eguchi and Hasegawa (2008).
- Storm 2002-5-7, a storm on soil of moderate antecedent water content, with relatively low intensity, yet likely to generate substantial preferential flow.
- Storm 1998-9-21, a storm on soil of moderate antecedent water content, comparable to that of 2002-5-7 but with higher weighted intensity.
- Storm 1998-2-20 (not in the tabulation of Eguchi and Hasegawa), a storm on soil of relatively low antecedent water content, with moderate intensity, likely to generate moderate preferential flow if the water content is a not major factor, but little preferential flow if it is.
- Storm 1998-9-30, a storm on soil of high antecedent water content, and of moderate intensity comparable to that of 1998-2-20.

Table 1 lists relevant parameters of these storms. Antecedent water content is taken as the measurement of average water content in the 0- to 1-m depth interval at the time precipitation starts. The total precipitation is the sum of rain gauge measurements R_i at half-hour intervals. Weighted intensity is from Eq. [19]. For four of these storms, PFF is the value tabulated by Eguchi and Hasegawa (2008, Table 2). For Storm 1998-02-20, which is not in that table on account of negligible preferential flow, PFF is calculated assuming the preferential flow is a small number between 0 and the detection limit of the method that Eguchi and Hasegawa used. Figures 3 through 5 show the distributions optimized by selecting the value of μ_g such that the model-computed value of PFF equals the data-based value in Column 5 of Table 1.

Table 1. Parameter values for five storms.

Storm	Antecedent θ	Total precipitation	Weighted q	PFF	μ_g	σ_g
		mm	mm/h		— mm/h —	
2001-10-01	0.575	119.8	8.86	0.407	5.08	3.00
2002-05-07	0.598	59.4	5.22	0.210	6.24	3.00
1998-09-21	0.599	53.4	14.95	0.376	9.47	3.00
1998-02-20	0.587	40.1	4.75	0.017	28.15	3.00
1998-09-30	0.622	37.6	4.57	0.652	1.10	3.00

Figure 3, for the storm highlighted by Eguchi and Hasegawa, shows the peak of the optimized $g(b)$ distribution at a value of b substantially less than the weighted intensity of the storm, so as to generate a substantial amount of preferential flow according to Eq. [15]. Figure 4, for storms of nearly equal antecedent water content but different weighted intensities, shows the storm of greater intensity generates more preferential flow. The different weighted intensity is the strongest visual difference in the two graphs. It is clear how the appropriately weighted integrations of the distribution function $g(b)$ represent the different portions of the distribution responsible for preferential flow for different storm intensities. Figure 5, for storms of nearly equal weighted intensity but different antecedent water content, shows the storm falling on the wetter soil generates more preferential flow. The $g(b)$ distributions are strikingly different in the two graphs, indicating that $g(b)$ depends sensitively on transient conditions of the soil. This result suggests that the matrix capacity dominates the antecedent moisture influence in this case; the wet matrix has less remaining capacity to absorb water, so more goes into preferential flow.

For the Storm 2001-10-10, sensitivity calculations (Fig. 6) show that the PFF is much more sensitive to μ_g than to σ_g. The

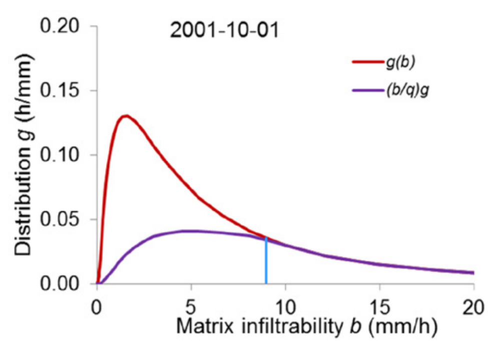

Fig. 3. Distribution function $g(b)$ optimized to fit the matrix–preferential flow partitioning observed by Eguchi and Hasegawa (2008) for Storm 2001-10-1.

sensitivity to σ_g does become substantial when its value is close to 1, but this exception occurs because $\sigma_g = 1$ is the unrealistic case of a totally uniform distribution of b, at which PFF = 0. Thus for a large range, including the value of 3 assumed in previous calculations, PFF determinations are largely unaffected by the value used for σ_g.

The parameter values, directions of sensitivities, and magnitudes of differences caused by the variables in these examples give a self-consistent picture that plausibly represents the infiltration and preferential flow characteristics of the site, according to expectations based on known effects of preferential flow. The framework's parameterization of the characteristic property distributions appropriately represent the effects of antecedent soil water and rainfall intensity, as seen especially in Fig. 4 and 5.

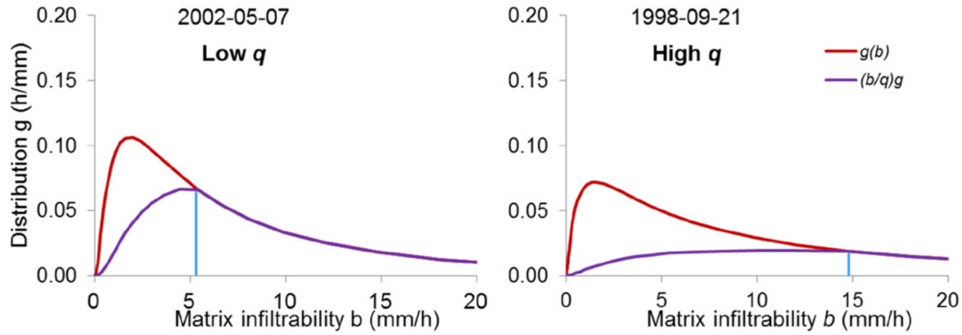

Fig. 4. Distribution functions $g(b)$ optimized to fit the matrix–preferential flow partitioning observed by Eguchi and Hasegawa (2008) for the Storms 2002-05-07 and 1998-09-21, both of which began when the 0- to 1-m average soil water content was 0.60. The weighted intensity of the two storms differed by nearly a factor of 3.

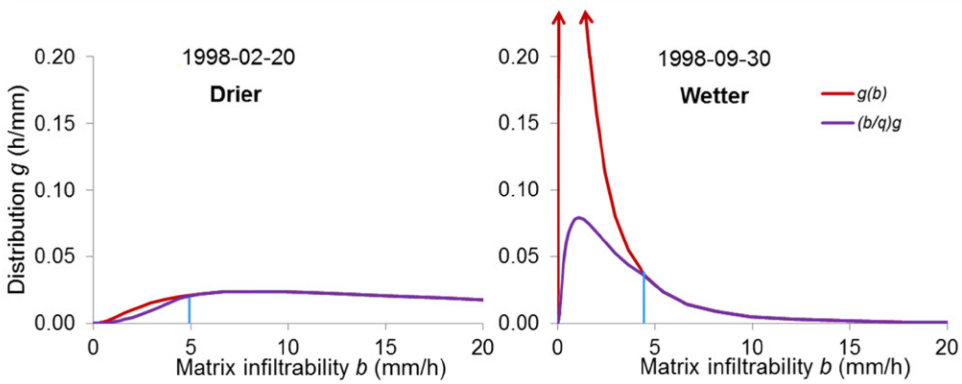

Fig. 5. Distribution functions $g(b)$ optimized to fit the matrix–preferential flow partitioning observed by Eguchi and Hasegawa (2008) for Storms 1998-02-20 and 1998-09-30, which had nearly equal weighted intensity. Storm 1998-02-20 began with a significantly lower 0- to 1-m average soil water content.

Test with Known Values of Matrix Infiltrability

Wilson and Luxmoore (1988) used tension infiltrometers, adjusted for application of water at a matric potential of −2 cm water, to measure soil matrix infiltrability at 37 locations over an area of 0.47 ha. In terms of cumulative probability, these measurements are plotted as the point symbols in Fig. 7. A lognormal distribution with $\mu_g = 62.4$ mm/h and $\sigma_g = 2.78$, shown in the figure as the curve of matching color, fits the data well. For comparison, the figure also includes cumulative lognormal distributions inferred from the Eguchi and Hasegawa measurements, for two storms of contrasting antecedent conditions. Figure 8 compares the corresponding $g(b)$ functions using the format of Fig. 2 through 5. Differences between the results of the two studies derive mainly from the greater prevailing infiltrability of the Tennessee soil. Results from the two storms of Eguchi and Hasegawa again illustrate the strong influence of antecedent moisture. Results for the storm on drier conditions at the Japanese site, reflecting the greater infiltrability in matrix material associated with greater capacity to absorb water, are closer to the Tennessee measurements. It still appears that, beyond effects of moisture conditions, the Tennessee soil has basic structural differences that give it generally greater infiltrability.

Based on calculations using Eq. [15] with these three distributions, Fig. 9 shows the model-predicted fraction of precipitation that becomes preferential flow. The results differ widely, showing that the characteristic matrix infiltrability distributions are a strong indicator of preferential flow behavior for a given site and conditions. When wet, the Japanese soil has the capability for very large amounts of preferential flow even at relatively modest intensities, likely having serious implications for recharging fluxes and solute

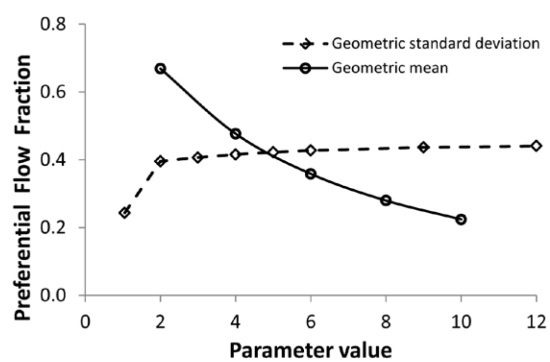

Fig. 6. Sensitivity of PFF to parameter values of the lognormal distribution. For tests with variation of the geometric mean, the geometric standard deviation was fixed at 3.0. For tests with variation of the geometric standard deviation, the geometric mean was fixed at 5.08 mm/h, the value optimized for Storm 2001-10-01.

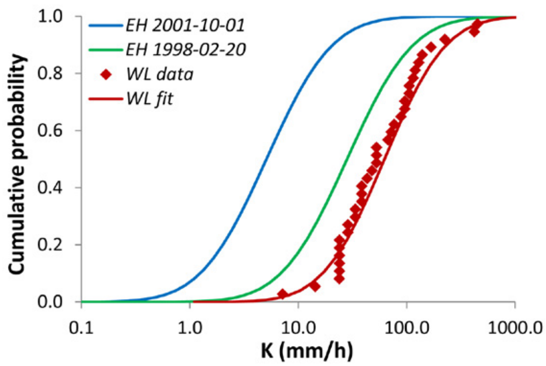

Fig. 7. Cumulative lognormal probability distributions for measurements and lognormal fit to data of Wilson and Luxmoore (1988), and inferred probability distributions for effective matrix conductivities for two storms in the data of Eguchi and Hasegawa (2008) with wet (Storm 2001-10-01) and dry (Storm 1998-02-20) antecedent conditions.

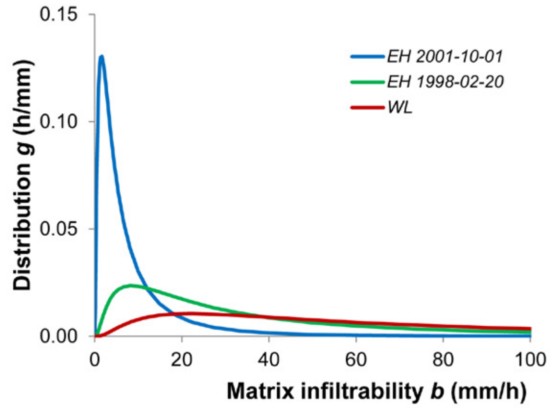

Fig. 8. Computed lognormal distributions of matrix infiltrability fit to data of Wilson and Luxmoore (1988) and optimized for two storms in the data of Eguchi and Hasegawa (2008).

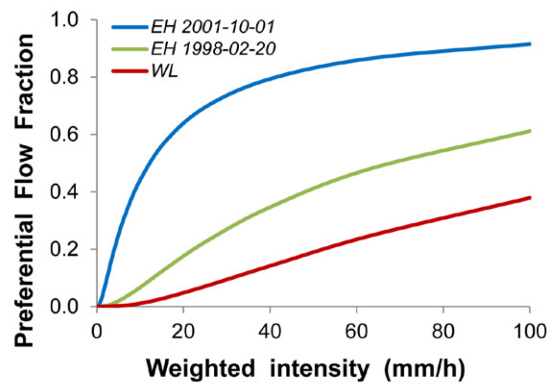

Fig. 9. Model-predicted fraction of precipitation going to preferential flow based on data of Wilson and Luxmoore (1988), and optimizations for two storms in the data of Eguchi and Hasegawa (2008).

transport. The Tennessee soil requires extremely high, and likely rare, storm intensity to generate a large proportion of preferential flow. Even in this matrix-conductive soil, however, there is an indication of preferential flow down to an intensity that is less, by a factor of 4, than the geometric mean matrix infiltrability. The predicted PFF is small at such low intensities, but could still have important consequences for contaminant transport.

Discussion

Characteristics and Interpretation

The model developed here represents soil properties governing macropore flow generation and partitioning based on the distribution of matrix infiltrability over the land surface. Optimized for data sets where both preferential and matrix flow have been measured, it computes the preferential–diffuse flow response to a given input flux. It does this through a quantification of the spatial variability of matrix infiltrability, leading to different proportions of preferential flow, diffuse flow, and runoff, for different intensities of precipitation.

The limited but successful tests performed with this model support various physical assumptions that underlie it. Chief among these is that in determining the timing and magnitude of macropore flow, the properties of the matrix material adjacent to a macropore are more important than those of the macropore itself. Values of the matrix infiltrability b relate to such properties as sorptivity, hydraulic conductivity, and hydrophobicity, and in effect also topography.

Postulating immediate macropore accessibility and continuum relations for heterogeneous soil properties, this model has no explicit reliance on macropore spacing. With these assumptions the model sidesteps any need to determine intermacropore distances or number-density of macropores. Avoiding this need is advantageous because estimation of such properties would require knowledge of *all* macropores within an area, which is difficult in practice, and also in principle, given the lack of a universally accepted definition of a macropore. The functional definition used here relies on hydraulic measurements rather than assessment by visual inspection or related means. While we do not yet know what range of pore aperture sizes this might include, available evidence, as noted in the introduction, suggests a broader inclusion than what is commonly employed.

The strong dependence of $g(b)$ on transient conditions of the soil is a useful insight into preferential flow behavior of the cases explored here. It confirms the results of other investigations that show antecedent soil moisture to influence preferential flow and provides a way to represent such dependences quantitatively. However, it complicates the problem of characterizing the matrix infiltrability distribution because one cannot assume a single determination of $g(b)$ would serve for a given field site. With additional research, it may be possible to parameterize a dependence on antecedent conditions. For example, μ_g might be found to vary systematically with soil water content. The distribution could then be scaled for this influence, giving it greater generality for the representation of a given site.

Utility

Results from this model clearly could be useful in combination with one of the many dual-domain models of subsurface flow (Šimůnek et al., 2003). The predicted matrix and macropore fluxes could directly specify inputs to diffuse and preferential domains. Given a finite valuation of *c*, the model could also compute runoff. It could be connected to existing runoff models, applying Eq. [9–11] to compute the contribution to runoff from water inputs that vary in magnitude and intensity.

Several choices made in this model's development facilitate its implementation. The model's continuum treatment of interacting processes avoids the need to specify the size of contributing area (here the EMA). The distribution functions $g(b)$ and $h(c)$ in effect represent the effects not only of matrix hydraulic conductivity but also the topography and the capacity and effective areal density of macropores. Greater topographic slope would cause smaller *b*. Greater spacing of macropores would cause smaller *c* or greater *b*. Lumping these acknowledged influences together means there are few parameters, appropriate for the sparseness of data typically available to implement a preferential flow model.

Depth-dependent factors, such as flowpath continuity, matrix water dynamics, and macropore–matrix interaction influence preferential flow, as observed, for example, by Kulli et al. (2003). Consequently, values of parameters such as μ_g and σ_g could vary with the choice of the depth where the partition of fluxes is calculated. This depth can be selected for a particular application. If the chosen depth is at the water table, the calculated preferential flow represents recharge. If the depth is at the bottom of the root zone, it represents the loss of water available to plants. Other possibilities include an emplaced flow detector, for comparison with measurements; a perched water body or other sensitive feature, for vulnerability assessment; a slippage plane, for landslides or related phenomena; and a soil pipe network, for subsurface stormflow.

Further Developments

One important extension of this research would be to adapt it for data in the form of a series of equal-length timesteps, as opposed to treating each storm as an integral unit. The weighted average of Eq. [19] includes some influence of the total amount, as well as the intensity, of precipitation in the storm. It does not support an analysis of the individual effects of such factors, however. Individual-timestep evaluation of the PFF would allow independent assessment of these factors. It would additionally allow more detailed predictions, as for the variation of PFF with rainfall intensity during a storm.

Simple extensions would be valuable for some cases. Macropore openings could constitute a finite portion of an REA, appropriate where numerous large pores open at the land surface. Spatial variability of water input could account for areally heterogeneous processes that occur with nonuniform surface cover, rainfall, irrigation, or snowmelt.

For the distribution functions $g(b)$ and $h(b,c)$, one can use a different parametric form, for example, the exponential form used by Hawkins and Cundy (1987). Moreover, the general framework is not limited to parameterized distributions; nonparametric functions would afford greater generality. Superpositions are also likely to be useful. For example, when there is a distinct categorization of surface types (e.g., leaf litter, bare soil, impermeable rock), one could use a different set of parameters for each type and superimpose the set of resulting curves. A particular use for this alternative would be to represent rock outcrops by adding a spike or delta-function near $b = 0$ to the distribution function.

Development of new capabilities requires more and better measured data concerning preferential flow and the conditions that influence it (e.g., Dusek et al., 2008). Few existing data sets quantify the partitioning into matrix and preferential flow as done by Eguchi and Hasegawa (2008). Beyond that, what is especially needed are field studies that measure both the distribution of matrix infiltrability and the quantity of preferential flow for a range of input and antecedent conditions. Such data sets would permit a full predictive test of models like the one developed here. Quantitative knowledge of the preferential proportion of flow is crucial; without it, development of models to predict when and how much preferential flow occurs would be impossible. Field experiments for this purpose need to be recognized as worth their cost, because of the great importance of preferential flow to major problems of water supply and contamination and the inability of current science to predict it reliably.

Conclusions

This paper presents a process-level characterization of macropore-flow initiation based on the principle that preferential flow can be predicted from the distribution of matrix infiltrability, developed into a framework for quantifying the partition of unsaturated flow into diffuse and preferential components. Hydraulic properties of soil matrix material, not the preferential flow paths themselves, are the main controlling influence. Quantification of the heterogeneity of matrix hydraulic properties is essential to the relationship between the amount of preferential flow and the characteristics of rainfall, irrigation, or other water inputs. A central feature is the representation of heterogeneous soil properties at a mesoscale that encompasses many micropores but is smaller than the REA that would be appropriate for determination of traditional infiltrability.

Few data sets have enough of the measurements needed for testing this framework. It has been tested with inverse calculation of model parameters based on the extensive multicomponent data set of Eguchi and Hasegawa (2008), showing that the framework quantifies the distribution of infiltrabilities that control macropore flow. Infiltrability measurements by Wilson and Luxmoore (1988) allow additional testing with forward calculation of parameters. The results correspond well to the measured data and general expectations based on effects of preferential flow, giving a self-consistent picture that plausibly represents infiltration and preferential flow. The characteristic matrix infiltrability distributions are a strong indicator of preferential flow behavior for a given site and conditions and appropriately represent effects of antecedent soil water and rainfall intensity.

This framework has immediate value for discerning the sensitivity of preferential flow to factors like soil wetness and precipitation intensity. Such studies, though difficult because of the diversity of factors that influence preferential flow, are a critical need in soil science and hydrology, intensified by the imperative to predict consequences of a changing climate. Ultimately, and especially as better field measurements become available, the framework presented in this paper would be valuable for predicting the occurrence and quantity of preferential flow.

Acknowledgments

I am grateful to Sadao Eguchi for providing detailed data in tabular form. Natalie Leibovitz and Zhengzheng Qin carried out many of the calculations needed for development and testing of the model presented here. The Hydrologic Research and Development Program and the National Research Program of the USGS provided support for this research.

References

Andreini, M.S., and T.S. Steenhuis. 1990. Preferential paths of flow under conventional and conservation tillage. Geoderma 46:85–102. doi:10.1016/0016-7061(90)90009-X

Aubertin, G.M. 1971. Nature and extent of macropores in forest soils and their influence on subsurface water movement. Research Paper NE-192. USDA Forest Service. Upper Darby, PA.

Beven, K., and P. Germann. 1982. Macropores and water flow in soils. Water Resour. Res. 18:1311–1325. doi:10.1029/WR018i005p01311

Bouma, J. 1981. Comment on “Micro-, Meso-, and Macroporosity of Soil”. Soil Sci. Soc. Am. J. 45(6):1244–1245. doi:10.2136/sssaj1981.03615995004500060050x

Bronstert, A. 1999. Capabilities and limitations of detailed hillslope hydrological modelling. Hydrol. Processes 13(1):21–48. doi:10.1002/(SICI)1099-1085(199901)13:1<21::AID-HYP702>3.0.CO;2-4

Bronstert, A., and E.J. Plate. 1997. Modelling of runoff generation and soil moisture dynamics for hillslopes and micro-catchments. J. Hydrol. 198(1–4):177–195. doi:10.1016/S0022-1694(96)03306-9

Cey, E.E., and D.L. Rudolph. 2009. Field study of macropore flow processes using tension infiltration of a dye tracer in partially saturated soils. Hydrol. Processes 23:1768–1779. doi:10.1002/hyp.7302

Coppola, A., H.H. Gerke, A. Comegna, A. Basile, and V. Comegna. 2012. Dual-permeability model for flow in shrinking soil with dominant horizontal deformation. Water Resour. Res. 48(8). doi:10.1029/2011WR011376

Dragila, M.I., and N. Weisbrod. 2003. Parameters affecting maximum fluid transport in large aperture fractures. Adv. Water Resour. 26(12):1219–1228. doi:10.1016/j.advwatres.2003.09.002

Dusek, J., H.H. Gerke, and T. Vogel. 2008. Surface boundary conditions in two-dimensional dual-permeability modeling of tile drain bromide leaching. Vadose Zone J. 7(4):1287–1301. doi:10.2136/vzj2007.0175

Eguchi, S., and S. Hasegawa. 2008. Determination and characterization of preferential water flow in unsaturated subsoil of Andisol. Soil Sci. Soc. Am. J. 72(2):320–330. doi:10.2136/sssaj2007.0042

Gerke, H.H. 2006. Preferential flow descriptions for structured soils. J. Plant Nutr. Soil Sci. 169(3):382–400. doi:10.1002/jpln.200521955

Germann, P.F., and D. Hensel. 2006. Poiseuille flow geometry inferred from velocities of wetting fronts in soils. Vadose Zone J. 5(3):867–876. doi:10.2136/vzj2005.0080

Hallett, P.D., N. Nunan, J.T. Douglas, and I.M. Young. 2004. Millimeter-scale spatial variability in soil water sorptivity. Soil Sci. Soc. Am. J. 68(2):352–358. doi:10.2136/sssaj2004.3520

Hardie, M., S. Lisson, R. Doyle, and W. Cotching. 2013. Determining the frequency, depth and velocity of preferential flow by high frequency soil moisture monitoring. J. Contam. Hydrol. 144(1):66–77. doi:10.1016/j.jconhyd.2012.10.008

Hawkins, R.H., and T.W. Cundy. 1987. Steady-state analysis of infiltration and overland flow for spatially varied hillslopes. J. Am. Water Resour. Assoc. 23(2):251–256. doi:10.1111/j.1752-1688.1987.tb00804.x

Hendrickx, J.M.H., and M. Flury. 2001. Uniform and preferential ñow mechanisms in the vadose zone. In: National Research Council, editors, Conceptual models of flow and transport in the fractured vadose zone. National Academy Press, Washington, DC. p. 149–187.

Heppell, C.M., F. Worrall, T.P. Burt, and R.J. Williams. 2002. A classification of drainage and macropore flow in an agricultural catchment. Hydrol. Processes 16(1):27–46. doi:10.1002/hyp.282

Hincapié, I.A., and P.F. Germann. 2009. Abstraction from infiltrating water content waves during weak viscous flows. Vadose Zone J. 8(4):891–901. doi:10.2136/vzj2009.0003

Jarvis, N.J. 2007. A review of non-equilibrium water flow and solute transport in soil macropores: Principles, controlling factors and consequences for water quality. Eur. J. Soil Sci. 58(3):523–546. doi:10.1111/j.1365-2389.2007.00915.x

Jarvis, N., J. Koestel, I. Messing, J. Moeys, and A. Lindahl. 2013. Influence of soil, land use and climatic factors on the hydraulic conductivity of soil. Hydrol. Earth Syst. Sci. 17(12):5185–5195. doi:10.5194/hess-17-5185-2013

Kätterer, T., B. Schmied, K.C. Abbaspour, and R. Schulin. 2001. Single- and dual-porosity modelling of multiple tracer transport through soil columns–effects of initial moisture and mode of application. Eur. J. Soil Sci. 52(1):25–36. doi:10.1046/j.1365-2389.2001.00355.x

Kohler, A., K.C. Abbaspour, M. Fritsch, and R. Schulin. 2003. Using Simple Bucket Models to Analyze Solute Export to Subsurface Drains by Preferential Flow. Vadose Zone J. 2(1):68–75. doi:10.2136/vzj2003.0068

Kulli, B., M. Gysi, and H. Flühler. 2003. Visualizing soil compaction based on flow pattern analysis. Soil Tillage Res. 70(1):29–40. doi:10.1016/S0167-1987(02)00121-6

Kung, K.J.S. 1990. Preferential flow in a sandy vadose zone–1. Field observation. Geoderma 46(1):51–58. doi:10.1016/0016-7061(90)90006-U

Kung, K.-J.S., M. Hanke, C.S. Helling, E.J. Kladivko, T.J. Gish, T.S. Steenhuis, and D.B. Jaynes. 2005. Quantifying pore-size spectrum of macropore-type preferential pathways. Soil Sci. Soc. Am. J. 69(4):1196–1208. doi:10.2136/sssaj2004.0208

Kung, K.-J.S., E.J. Kladivko, C.S. Helling, T.J. Gish, T.S. Steenhuis, and D.B. Jaynes. 2006. Quantifying the pore size spectrum of macropore-type preferential pathways under transient flow. Vadose Zone J. 5(3):978–989. doi:10.2136/vzj2006.0003

Langhans, C., G. Govers, and J. Diels. 2013. Development and parameterization of an infiltration model accounting for water depth and rainfall intensity. Hydrol. Processes 27(25):3777–3790. doi:10.1002/hyp.9491

Langhans, C., G. Govers, J. Diels, A. Leys, W. Clymans, A.V.d. Putte, and J. Valckx. 2011. Experimental rainfall–runoff data: Reconsidering the concept of infiltration capacity. J. Hydrol. 399(3–4):255–262. doi:10.1016/j.jhydrol.2011.01.005

Lipiec, J., A. Wójciga, and R. Horn. 2009. Hydraulic properties of soil aggregates as influenced by compaction. Soil Tillage Res. 103(1):170–177. doi:10.1016/j.still.2008.10.021

Miller, E.E., and R.D. Miller. 1956. Physical theory for capillary flow phenomena. J. Appl. Phys. 27(4):324–332. doi:10.1063/1.1722370

Mualem, Y. 1974. A conceptual model of hysteresis. Water Resour. Res. 10(3):514–520. doi:10.1029/WR010i003p00514

Nielsen, D.R., J.W. Biggar, and K.T. Erh. 1973. Spatial variability of field-measured soil-water properties. Hilgardia 42(7):215–259. doi:10.3733/hilg.v42n07p215

Nimmo, J.R. 2007. Simple predictions of maximum transport rate in unsaturated soil and rock. Water Resour. Res. 43(5). doi:10.1029/2006WR005372

Nimmo, J.R. 2010. Theory for source-responsive and free-surface film modeling of unsaturated flow. Vadose Zone J. 9(2):295–306. doi:10.2136/vzj2009.0085

Nimmo, J.R. 2012. Preferential flow occurs in unsaturated conditions. Hydrol. Processes 26(5):786–789. doi:10.1002/hyp.8380

Nimmo, J.R., and L. Mitchell. 2013. Predicting vertically nonsequential wetting patterns with a source-responsive model. Vadose Zone J. 12(4). doi:10.2136/vzj2013.03.0054

Nimmo, J.R., K.S. Perkins, K.M. Schmidt, D.M. Miller, J.D. Stock, and K. Singha. 2009. Hydrologic characterization of desert soils with varying degrees of pedogenesis. I. Field experiments evaluating plant-relevant soil-water behavior. Vadose Zone J. 8(2):480–495. doi:10.2136/vzj2008.0052

Patin, J., E. Mouche, O. Ribolzi, V. Chaplot, O. Sengtahevanghoung, K.O. Latsachak, B. Soulileuth, and C. Valentin. 2012. Analysis of runoff production at the plot scale during a long-term survey of a small agricultural catchment in Lao PDR. J. Hydrol. 426–427(0):79–92. doi:10.1016/j.jhydrol.2012.01.015

Perkins, K.S., J.R. Nimmo, C.E. Rose, and R.H. Coupe. 2011. Field tracer investigation of unsaturated zone flow paths and mechanisms in agricultural soils of northwestern Mississippi, USA. J. Hydrol. 396(1–2):1–11. doi:10.1016/j.jhydrol.2010.09.009

Philip, J.R. 1964. Similarity hypothesis for capillary hysteresis in porous materials. J. Geophys. Res. 69(8):1553–1562. doi:10.1029/JZ069i008p01553

Pruess, K. 1999. A mechanistic model for water seepage through thick unsaturated zones in fractured rocks of low matrix permeability. Water Resour. Res. 35(4):1039–1051. doi:10.1029/1998WR900100

Quisenberry, V.L., and R.E. Phillips. 1976. Percolation of surface-applied water in the field. Soil Sci. Soc. Am. J. 40(4):484–489. doi:10.2136/sssaj1976.03615995004000040013x

Radulovich, R., P. Baveye, P. Sollins, and E. Solórzano. 1992. Bypass water flow through unsaturated microaggregated tropical soils. Soil Sci. Soc. Am. J. 56(3):721–726. doi:10.2136/sssaj1992.03615995005600030008x

Ritsema, C.J., and L.W. Dekker. 1995. Distribution flow—A general process in the top layer of water repellent soils. Water Resour. Res. 31(5):1187–1200. doi:10.1029/94WR02979

Ritsema, C.J., and L.W. Dekker. 1996. Water repellency and its role in forming preferred flow paths in soils. Aust. J. Soil Res. 34(4):475–487. doi:10.1071/SR9960475

Rosenbom, A.E., W. Brüsch, R.K. Juhler, V. Ernstsen, L. Gudmundsson, J. Kjær, F. Plauborg, R. Grant, P. Nyegaard, and P. Olsen. 2010. The Danish Pesticide Leaching Assessment Programme monitoring results May 1999–June 2009. Geological Survey of Denmark and Greenland, Copenhagen.

Salve, R., D.M. Rempe, and W.E. Dietrich. 2012. Rain, rock moisture dynamics, and the rapid response of perched groundwater in weathered, fractured argillite underlying a steep hillslope. Water Resour. Res. 48(11). doi:10.1029/2012WR012583

Scotter, D.R., and P. Kanchanasut. 1981. Anion movement in a soil under pasture. Aust. J. Soil Res. 19(3):299–307. doi:10.1071/SR9810299

Shiozawa, S., and H. Fujimaki. 2004. Unexpected water content profiles under flux-limited one-dimensional downward infiltration in initially dry granular media. Water Resour. Res. 40(7). doi:10.1029/2003WR002197

Šimůnek, J., N.J. Jarvis, M.Th. van Genuchten, and A. Gärdenäs. 2003. Review and comparison of models for describing non-equilibrium and preferential flow and transport in the vadose zone. J. Hydrol. 272(1–4):14–35. doi:10.1016/S0022-1694(02)00252-4

Smith, R.E., and R.H.B. Hebbert. 1979. A Monte Carlo analysis of the hydrologic effects of spatial variability of infiltration. Water Resour. Res. 15(2):419–429. doi:10.1029/WR015i002p00419

Stone, J.J., G.B. Paige, and R.H. Hawkins. 2008. Rainfall intensity-dependent infiltration rates on rangeland rainfall simulator plots. Trans. ASABE 51(1):45–53. doi:10.13031/2013.24226

Su, G.W., J.T. Geller, K. Pruess, and F. Wen. 1999. Experimental studies of water seepage and intermittent flow in unsaturated, rough-walled fractures. Water Resour. Res. 35(4):1019–1037. doi:10.1029/1998WR900127

Su, G.W., J.R. Nimmo, and M.I. Dragila. 2003. Effect of isolated fractures on accelerated flow in unsaturated porous rock. Water Resour. Res. 39(12). doi:10.1029/2002WR001691

Thomas, G.W., and R.E. Phillips. 1979. Consequences of water movement in macropores. J. Environ. Qual. 8(2):149–152. doi:10.2134/jeq1979.00472425000800020002x

Tokunaga, T.K., J. Wan, and S.R. Sutton. 2000. Transient film flow on rough fracture surfaces. Water Resour. Res. 36(7):1737–1746. doi:10.1029/2000WR900079

Tuller, M., and D. Or. 2001. Hydraulic conductivity of variably saturated porous media—Film and corner flow in angular pore space. Water Resour. Res. 37(5):1257–1276. doi:10.1029/2000WR900328

Tyner, J.S., W.C. Wright, and R.E. Yoder. 2007. Identifying long-term preferential and matrix flow recharge at the field scale. Trans. ASABE 50(6):2001–2006. doi:10.13031/2013.24103

van Schaik, N.L.M.B. 2009. Spatial variability of infiltration patterns related to site characteristics in a semi-arid watershed. Catena 78(1):36–47. doi:10.1016/j.catena.2009.02.017

van Schaik, N.L.M.B., S. Schnabel, and V.G. Jetten. 2008. The influence of preferential flow on hillslope hydrology in a semi-arid watershed (in the Spanish Dehesas). Hydrol. Processes 22(18):3844–3855. doi:10.1002/hyp.6998

Villholth, K.G., and K.H. Jensen. 1998. Flow and transport processes in a macroporous subsurface-drained glacial till soil. II. Model analysis. J. Hydrol. 207:121–135. doi:10.1016/S0022-1694(98)00130-9

Villholth, K.G., K.H. Jensen, and J. Fredericia. 1998. Flow and transport processes in a macroporous subsurface-drained glacial till soil. I. Field investigations. J. Hydrol. 207:98–120. doi:10.1016/S0022-1694(98)00129-2

Weiler, M. 2005. An infiltration model based on flow variability in macropores: Development, sensitivity analysis and applications. J. Hydrol. 310(1–4):294–315. doi:10.1016/j.jhydrol.2005.01.010

Weiler, M., and F. Naef. 2003. Simulating surface and subsurface initiation of macropore flow. J. Hydrol. 273(1–4):139–154. doi:10.1016/S0022-1694(02)00361-X

Wilson, G.V., and R.J. Luxmoore. 1988. Infiltration, macroporosity, and mesoporosity distributions on two forested watersheds. Soil Sci. Soc. Am. J. 52(2):329–335. doi:10.2136/sssaj1988.03615995005200020005x

Yang, Y.-W., G. Zografi, and E.E. Miller. 1988. Capillary flow phenomena and wettability in porous media–II. Dynamic flow studies. J. Colloid Interface Sci. 122(1):35–46. doi:10.1016/0021-9797(88)90285-8